

Correlations with a high- p_T trigger over a broad η range

Gábor I. Veres* for the PHOBOS Collaboration

Eötvös Loránd University, Budapest, Hungary

E-mail: gabor.veres@cern.ch

A selection of recent experimental results from the PHOBOS Collaboration on correlations that involve high transverse momentum ‘trigger’ particles in nuclear collisions is presented. It is known that the inclusive yields of charged particles and comparisons between nuclear and elementary collisions already reveal a large amount of parton energy loss in the hot and dense strongly interacting medium. To analyze the nature of the energy loss in more detail, a measurement of pseudorapidity ($\Delta\eta$) and azimuthal angle ($\Delta\phi$) correlations between high transverse momentum charged hadrons ($p_T > 2.5$ GeV/c) and all associated charged particles is presented in the short-range (small $\Delta\eta$) and long-range (large $\Delta\eta$) categories, over a continuous detector acceptance that covers $-4 < \Delta\eta < 2$. Various near- and away-side features of the correlation structure are discussed as a function of centrality in Au+Au collisions at $\sqrt{s_{NN}} = 200$ GeV. The results provide new information about the longitudinal ($\Delta\eta$) extent of the near-side ‘ridge’ structure, first observed by the STAR Collaboration over a narrower η range. In central Au+Au collisions the ridge structure extends to at least $\Delta\eta = 4$, and its strength diminishes towards peripheral collisions.

High- p_T Physics at the LHC - Tokaj’08

16-19 March 2008

Tokaj, Hungary

*Speaker.

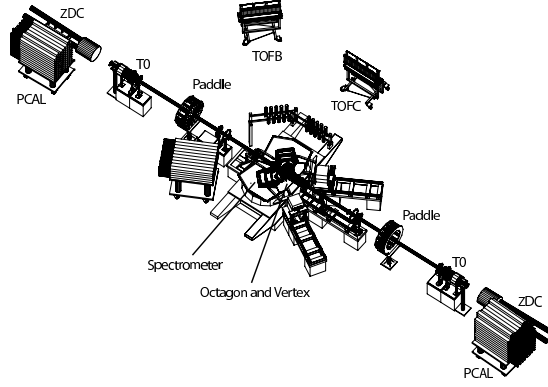


Figure 1: The schematic view of the PHOBOS detector system.

1. Introduction

The general goal of the experimental studies of high energy nuclear collisions is to create a new phase of matter at very high density and temperature, where hadrons are replaced by partons as relevant degrees of freedom. The conditions in the created medium are thought to be similar to those in the early Universe well before the nucleosynthesis. A large part of the experimental evidence that a new form of matter is created in these collisions comes from measurements related to particles with high transverse momentum. Interactions between those particles and the produced medium is a useful tool to reveal certain features of the elusive new form of matter.

After a brief description of the PHOBOS detector system, two particular methods to study these interactions will be presented. The first one is the comparison of inclusive charged hadron transverse momentum spectra between elementary and nuclear collisions. The second approach utilizes the large acceptance of the PHOBOS apparatus to explore the correlation between energetic charged particles and all the other particles in the event, revealing more details about the nature of both the partonic energy loss and the dense medium itself.

2. The PHOBOS detector system

The PHOBOS apparatus consists of highly segmented silicon sensors, various scintillator and Cherenkov detector arrays and calorimeters. Fig. 1 shows the schematic drawing of the layout.

The collision point is surrounded by the two arms of the multi-layered silicon Spectrometer, that are placed in a double dipole magnetic field. They have a pseudorapidity acceptance for charge particle tracking and momentum determination of $0 < \eta < 1.5$, although their azimuthal angle coverage is limited. The multiplicity array is a single layer of silicon detectors, and has two structural parts: a tubular Octagon detector with almost full azimuthal coverage over $|\eta| < 3.2$, and six silicon Ring detectors, perpendicular to the beam, extending the coverage to $|\eta| = 5.4$.

The scintillator Paddle detectors are two segmented disks on both sides of the interaction point, covering the $3 < |\eta| < 4.5$ range. They are used to trigger on collisions, and to sort the triggered heavy ion events into centrality classes that are based on the total amount of energy deposited in the scintillators. Further details of the detector system can be found in [1].

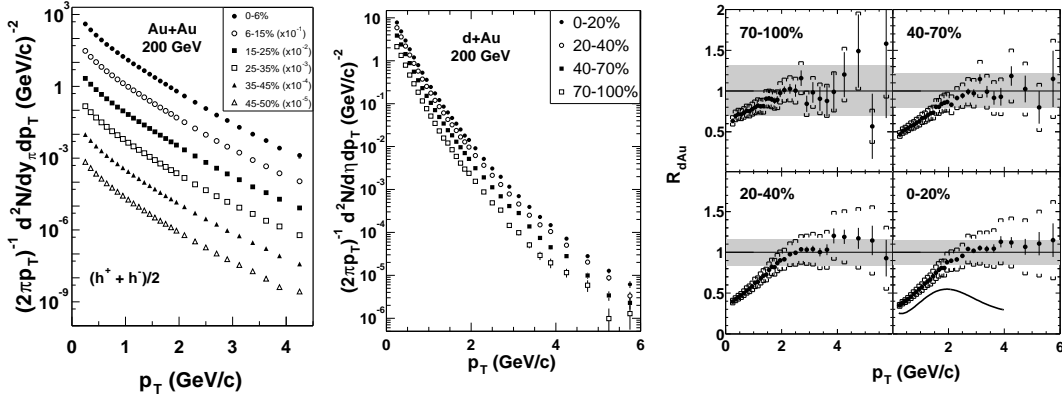


Figure 2: Inclusive charged particle transverse momentum spectra measured in Au+Au (left panel) and d+Au (center panel) collisions at 200 GeV/nucleon center-of-mass energy. Nuclear modification factors (right panel), R_{dAu} , as a function of transverse momentum for charged hadrons in four centrality classes of d+Au collisions at $\sqrt{s_{NN}} = 200$ GeV. The solid line on the bottom right subpanel (most central collisions) shows the R_{AuAu} nuclear modification factor for Au+Au collisions at the same collision energy. Error bars stand for statistical, brackets for systematic errors. The gray bands are scale errors shared by all data points.

3. Correlations with a high- p_T particle

One of the most important discoveries of the Relativistic Heavy Ion Collider (RHIC) is that high-energy partons interact strongly and lose a significant fraction of their energy as they traverse the medium produced in nuclear collisions. The energy loss can be inferred from the measurement of charged hadron transverse momentum spectra. Fig. 2 shows examples of charged hadron spectra measured with the PHOBOS Spectrometer at $\sqrt{s_{NN}} = 200$ GeV collision energy, in Au+Au [2] and d+Au [3] collisions. In both cases, the spectra are measured in various classes of collision centrality, labelled with the percentage interval of the total inelastic cross section. In the case of the d+Au data, a special high- p_T trigger was utilized to extend the statistical p_T reach.

The significant difference between the shapes of the p_T -spectra in Au+Au and d+Au collisions is visible on Fig. 2. A better way to quantify these differences is to compare these complex systems to a reference of proton-proton collisions, by taking the ratio of the transverse momentum spectra. These ratios, the nuclear modification factors, are defined as:

$$R_{AA}(p_T) = \frac{\sigma_{pp}^{inel}}{\langle N_{coll} \rangle} \frac{d^2 N_{AA}/dp_T d\eta}{d^2 \sigma_{pp}/dp_T d\eta}, \quad (3.1)$$

where $\langle N_{coll} \rangle$ is the mean number of binary nucleon-nucleon collisions in the given centrality class of the data. Without any nuclear effects, $R_{AA} = 1$ is expected at high p_T . The right panel of Fig. 2 shows the nuclear modification factors, R_{dAu} , for charged hadrons in four centrality classes of d+Au collisions at $\sqrt{s_{NN}} = 200$ GeV as a function of transverse momentum [3]. The R_{AuAu} nuclear modification factor for Au+Au events at the same energy is also plotted with the solid line on the bottom right panel (corresponding to the most central collisions). While there is a strong suppression (by a factor of 4-5) of the hadron yields at high p_T in the heavy ion data, the R_{dAu} factors are around (or slightly exceed) unity for $p_T > 3$ GeV/c. This result is evidence that the

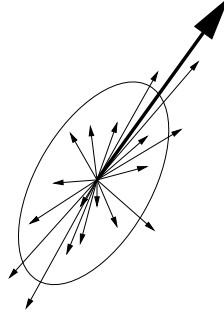


Figure 3: A sketch of the two particle azimuthal angle correlation measurement. The thick arrow represents the high- p_T trigger particle, while the other arrows depict associated particles, in a plane perpendicular to the beam. The ellipse symbolizes the azimuthal angle distribution (averaged over many events).

observed suppression is caused by a final state effect in heavy ion collisions, which is connected to the presence of the high density medium. Similar results are also obtained by the PHENIX and STAR experiments at RHIC [4, 5].

The effect of the large amount of energy lost by energetic partons traversing the medium is also observed in azimuthal correlations, where back-to-back high- p_T particles disappear in central Au+Au collisions [6]. In these measurements, a high- p_T trigger particle is selected from a given heavy ion event, and some, or all of the other particles in the same event are called associated particles, as sketched in Fig. 3. The correlation between the direction of the trigger and associated particles is measured, usually both in the azimuthal angle (ϕ) and pseudorapidity (η) direction.

For associated particles selected to have high momentum, the behavior is consistent with the surface emission of jets, caused by the presence of an opaque medium that completely absorbs those jets directed at the interior.

However, the energy and momentum of the away-side jet must be present in the final state due to the energy-momentum conservation, and it is necessarily carried by the associated particles. Therefore, there is a strong motivation to study the correlations between high- p_T triggers and lower p_T associated particles. At mid-rapidity, data collected at RHIC show several nontrivial features in the structure of those correlation functions. In addition to a broadening of the reemergent away-side structure relative to p+p [7, 8], a striking enhancement in the correlation near $\Delta\phi = 0$ is also observed. This structure extends over several units of pseudorapidity, and has been called the ‘ridge’ [9]. Although the ridge at mid-rapidity has been qualitatively described by a diverse assortment of proposed mechanisms using various theoretical approaches [10, 11, 12, 13, 14, 15, 16, 17], the precise origin of the structure is still not well understood. In this context, the goal of the PHOBOS collaboration is to use the uniquely broad pseudorapidity acceptance of the PHOBOS multiplicity detector array to measure the ridge structure (and its dependence on event centrality) at large relative pseudorapidity ($\Delta\eta$), and therefore constrain the possible interpretations of particle production correlated with high- p_T trigger particles.

The silicon Spectrometer was used to select charged trigger tracks with $p_T > 2.5$ GeV/c within the longitudinal acceptance of $0 < \eta^{trig} < 1.5$. Associated particles that are able to traverse the beryllium beam-pipe ($p_T > 4$ MeV/c at $\eta \approx 3$, $p_T > 35$ MeV/c at $\eta \approx 0$) are detected in the single-layered silicon Octagon detector, covering the $|\eta| < 3$ range. There is no additional p_T selection

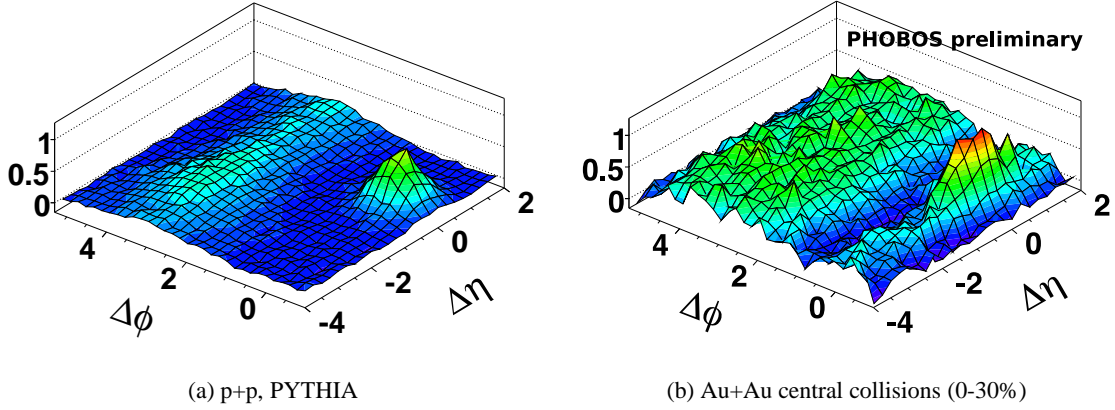


Figure 4: Correlated yield per trigger particle using $p_T^{trig} > 2.5$ GeV/c, as a function of $\Delta\eta$ and $\Delta\phi$ for 200 GeV (a) p+p events generated by PYTHIA and (b) for Au+Au collisions measured by PHOBOS.

for associated particles. Due to the design of the Octagon, there are certain inactive windows in the detector, but those can be filled to a large extent, using the first layers of the Vertex detector and the Spectrometer arms.

The conditional yield of charged particles per trigger is calculated by taking the raw per-trigger distribution of same-event pairs, $s(\Delta\phi, \Delta\eta)$, and dividing by the raw distribution of mixed-event pairs (the ‘background’), $b(\Delta\phi, \Delta\eta)$, to remove random coincidences and effects of the detector acceptance. This ratio is calculated in 1 mm wide bins of vertex position along the beam-line, v_z , and averaged over the range $-15 < v_z < 10$ cm:

$$\frac{1}{N_{trig}} \frac{d^2 N_{ch}}{d\Delta\phi d\Delta\eta} = B(\Delta\eta) \cdot \left[\frac{s(\Delta\phi, \Delta\eta)}{b(\Delta\phi, \Delta\eta)} - a(\Delta\eta) [1 + 2V(\Delta\eta) \cos(2\Delta\phi)] \right] \quad (3.2)$$

The last term in Eq. 3.2 is due to the collective effect in heavy ion collisions called elliptic flow: the azimuthal angle distribution of produced particles is not uniform, but has a cosine-like modulation (to first approximation) with a strength quantified by its second Fourier-coefficient, v_2 . This distribution is symbolized by the ellipse in Fig. 3. The orientation of the ellipse is correlated with the impact parameter vector in the given nuclear collision.

Elliptic flow is completely erased in the mixing of tracks and hits (associated particles) from different events, thus the background will be uniformly distributed in $\Delta\phi$. However, both the trigger and the associated particles will be distributed according to the above non-uniform distribution, thus the same-event pairs will also show a remaining flow modulation, which has to be subtracted from the correlation measurement. The remaining second-order modulation is denoted by $V(\Delta\eta)$, and can be approximated by the product of $\langle v_2^{trig} \rangle$ and $\langle v_2^{assoc} \rangle$. The magnitude of the elliptic flow is calculated according to a parameterization based on published PHOBOS measurements of v_2 as a function of N_{part} , p_T , and η in Au+Au events at 200 GeV, assuming a factorized form [18].

The v_2 of the trigger tracks is corrected for occupancy effects in the Spectrometer, and the v_2 of the associated hits is corrected for secondaries. Both of these effects tend to suppress the magnitude of the observed v_2 . Finally, the scale factor $a(\Delta\eta)$ in Eq. 3.2 is introduced to account for the small difference in multiplicity, caused by the trigger bias, between signal and mixed-event distributions

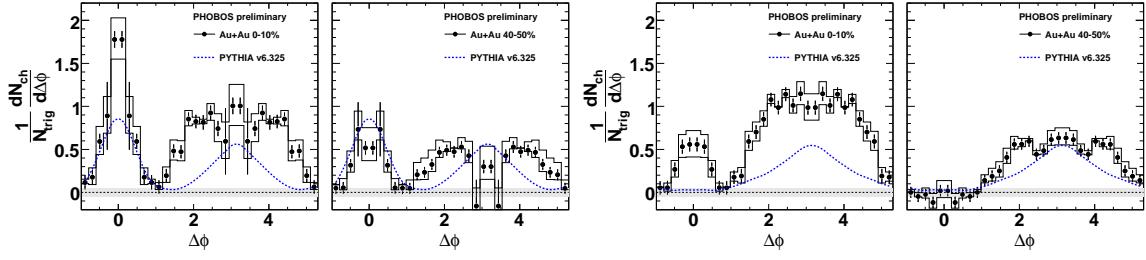


Figure 5: Per-trigger correlated yield for central (0-10%, first and third panel) and semi-peripheral (40-50%, second and fourth panel) Au+Au collisions at $\sqrt{s_{NN}} = 200$ GeV as a function of the $\Delta\phi$ angular distance between the trigger and associated particles. The first two panels show the short range ($|\Delta\eta| < 1$) part of the correlation; the last two panels show the long range part ($-4 < \Delta\eta < -2$). The dashed line represents the correlation for p+p collisions from PYTHIA at the same energy.

for a given centrality class. It is calculated using the zero yield at minimum (ZYAM) method [19] and only differs from unity by a few percent in all cases considered. The ZYAM method ensures that the subtracted correlation function is nonnegative, and has a minimum value of zero. $B(\Delta\eta)$ is simply the corrected, published single-particle distribution ($dN/d\eta$) [20] convoluted with the properly normalized η distribution of trigger particles.

The dominant systematic error in the correlation analysis comes from the uncertainty in estimating the magnitude of the flow modulation, $\langle v_2^{trig} \rangle \langle v_2^{assoc} \rangle$. The uncertainty on this estimate is typically on the order of 15-20%, and in central collisions it reaches 50%, but there the subtracted flow modulation is quite small compared to the jet correlation obtained after the subtraction.

To highlight the effects of the hot, dense medium on correlated particle production, the PHOBOS Au+Au data is compared to p+p events simulated with the PYTHIA event generator [21]. The p+p correlation is shown in Fig. 4(a), and its prominent features are a jet-fragmentation peak centered about $\Delta\eta \approx \Delta\phi \approx 0$ and an away-side structure centered at $\Delta\phi \approx \pi$ that has similar width in $\Delta\phi$ but is much more extended in $\Delta\eta$. The elongated longitudinal nature of this away-side bump is expected, since the hard scattering that has led to the appearance of the high- p_T trigger particle can involve partons with very different longitudinal momentum.

In central Au+Au collisions, particle production correlated with a high- p_T trigger is strongly modified with respect to the p+p events, as shown in Fig. 4(b). Not only is the away-side structure spectacularly broader in $\Delta\phi$, the near-side peak now sits on a pedestal, an unmistakable ridge of correlated partners extending continuously all the way to the edge of the detector acceptance at $\Delta\eta = 4$. The observed elongation of the near-side ridge (in η) is more challenging to interpret.

To examine the centrality dependence of the correlation structure, the correlated yield of associated particles as a function of $\Delta\phi$ was plotted in Fig. 5 in two $\Delta\eta$ slices: the first two panels show the short range correlations defined as $|\Delta\eta| < 1$, while the third and fourth panels show long range correlations in the $-4 < \Delta\eta < -2$ interval. Data from central Au+Au events (0-10%) are plotted in the first and third panel, and semi-peripheral data (40-50%) can be seen in the second and fourth panel. For comparison, the results from p+p events generated by PYTHIA are also depicted by dashed lines. One can conclude that in semi-peripheral Au+Au events the near-side structure is compatible with the p+p events, while the away-side broadening is still visible. However, for central Au+Au events both structures exceed in magnitude those observed in the p+p events, and

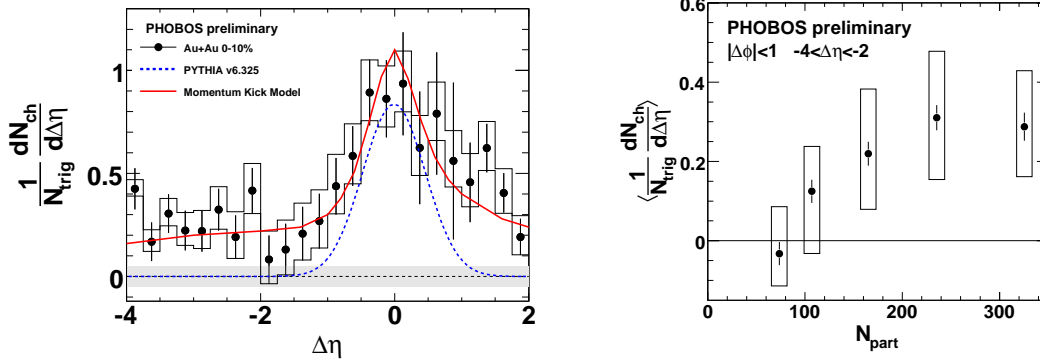


Figure 6: Left: per-trigger correlated yield for central Au+Au events (0-10%) integrated over the near side ($|\Delta\phi| < 1$) compared to PYTHIA (dashed line) and to the momentum kick model prediction [22] (solid line) as a function of $\Delta\eta$. Boxes represent the systematic uncertainty. Right: average yield of the ridge as a function of N_{part} in the $-4 < \Delta\eta < -2$ range. Boxes represent the systematic errors.

there is a near-side peak even at large $\Delta\eta$.

To examine the near-side structure more closely, the correlated yield is integrated over the $|\Delta\phi| < 1$ region and plotted as a function of $\Delta\eta$ on the left panel of Fig. 6 for the 10% most central Au+Au collisions. There is a significant and relatively $\Delta\eta$ -independent correlated yield of about 0.3 particles per unit of pseudorapidity, even far away from the trigger. The prediction of the momentum kick model [22], which has been tuned to results of the STAR experiment with $|\eta^{\text{assoc}}| < 1$ [8] and $2.7 < |\eta^{\text{assoc}}| < 3.9$ [23], is found to agree well with the experimental data. The momentum kick model postulates a parton rapidity distribution at the time of the jet-parton collision that is much broader than the rapidity distribution of final state hadrons. This suggests that the extent of the ridge is sensitive to the earliest moments of the Au+Au collision, and can be used as a probe of the initial parton rapidity distributions [24]. Several other interpretations of the ridge phenomenon have also been proposed [10, 11, 12, 13, 14, 15, 16, 17].

Finally, the centrality dependence of the average ridge yield far away from the trigger ($-4 < \Delta\eta < -2$) is shown on the right panel of Fig. 6. The ridge yield decreases towards more peripheral collisions, until it vanishes and becomes consistent with zero in the most peripheral bin analyzed (40-50% centrality). While the present systematic errors do not exclude a smooth disappearance of the ridge yield as one approaches p+p collisions, these preliminary data suggest the ridge may have already disappeared by the centrality class with $\langle N_{\text{part}} \rangle = 80$.

4. Summary

Recent experimental results from the PHOBOS experiment at RHIC have been discussed, related to the properties of the medium created in ultra-relativistic heavy ion collisions. Charged hadron transverse momentum spectra are sensitive to the sizeable energy loss suffered by partons in this medium; nuclear modification factors clearly show the quenching effect.

Preliminary PHOBOS measurements of the ridge in the correlation structure between high- p_T trigger particles and inclusive associated particles at small $\Delta\phi$ have been presented over a broad

range of $\Delta\eta$. The fact that in central collisions the ridge extends to at least four units of rapidity away from the trigger is a quantitative challenge to theories that strive to explain the nature of the jet-medium interaction. Further theoretical studies will be required to determine which proposed mechanisms are consistent with the broad extent of the ridge and its dependence on collision geometry.

5. Acknowledgements

This work was partially supported by U.S. DOE grants DE-AC02-98CH10886, DE-FG02-93ER40802, DE-FG02-94ER40818, DE-FG02-94ER40865, DE-FG02-99ER41099, and DE-AC02-06CH11357, by U.S. NSF grants 9603486, 0072204, and 0245011, by Polish MNiSW grant N N202 282234 (2008-2010), by NSC of Taiwan Contract NSC 89-2112-M-008-024, and by the Hungarian OTKA grant (F 049823) and the Zoltán Magyary Postdoctoral Fellowship.

References

- [1] Back B B *et al.* [PHOBOS] Nucl. Inst. Meth. A **499**, (2003) 603
- [2] Back B B *et al.* [PHOBOS] Phys. Lett. **B578**, (2004) 297
- [3] Back B B *et al.* [PHOBOS] Phys. Rev. Lett. **91**, (2003) 072302
- [4] Adler S S *et al.* [PHENIX] Phys. Rev. C **69**, (2004) 034910
- [5] Adams J *et al.* [STAR] Phys. Rev. Lett. **91**, (2003) 172302
- [6] Adler C *et al.* [STAR] Phys. Rev. Lett. **90**, (2003) 082302
- [7] Adare A *et al.* [PHENIX] Phys. Rev. C **77**, (2008) 011901(R)
- [8] Adams J *et al.* [STAR] Phys. Rev. Lett. **95**, (2005) 152301
- [9] Putschke J [STAR] J. Phys. G: Nucl. Part. Phys. **34**, (2007) S679
- [10] Armesto N, Salgado C and Wiedemann U Phys. Rev. Lett. **93**, (2004) 242301
- [11] Chiu C B and Hwa R C Phys. Rev. C **72**, (2005) 034903
- [12] Romatschke P Phys. Rev. C **75**, (2007) 014901
- [13] Majumder A, Müller B and Bass S A Phys. Rev. Lett. **99**, (2007) 042301
- [14] Shuryak E V Phys. Rev. C **76** (2007) 047901
- [15] Pantuev V S *Preprint* hep-ph/0710.1882 (2007)
- [16] Wong C Y *Preprint* hep-ph/0712.3282 (2007)
- [17] Dumitru A, Gelis F, McLerran L, Venugopalan R *Preprint* hep-ph/0804.3858 (2008)
- [18] Back B B *et al.* [PHOBOS] Phys. Rev. C **72**, (2005) 05190
- [19] Ajitanand N N *et al.* Phys. Rev. C **72**, (2005) 011902(R)
- [20] Back B B *et al.* [PHOBOS] Phys. Rev. Lett. **91**, (2003) 052303
- [21] Sjöstrand T *et al.* Computer Phys. Commun. **135**, (2001) 238, PYTHIA 6.325, default settings.
- [22] Wong C Y, private communications.
- [23] Molnar L [STAR] J. Phys. G: Nucl. Part. Phys. **34**, (2007) S593
- [24] Wong C Y Phys. Rev. C **76**, (2007) 054908